

and together they yield the 3-D correlation between any two arbitrary functions. Implementing a 3-D Fourier transform in the first stage by electro-optical means is the key concept of the proposed system. Based on the convolution theorem, an additional 3-D Fourier transform yields the desired 3-D correlation result.

In our example, the input scene contains four vehicles as shown in Figure 1. One of them, the reference, is located in the right side of the scene and is identical to two cars from the left group of the three vehicles used here as the observed objects. Note that the two lower vehicles are located in front of the reference, whereas the upper vehicle is behind it. The system should recognize the two cars that are identical to the reference and ignore the other vehicle. In this experiment, a single camera was shifted along the x-axis to 24 equal displacements, 12 for each side. Each projection was recorded by the camera and Fourier transformed. The intensity of each 2-D Fourier transform was stored in the computer.

3-D plots of the output space are shown in the lower part of Figure 1. Each 3-D plot presents the transverse intensity distribution at some  $z_0$  along the longitudinal axis. The two strong correlation peaks on planes  $z_0 = -2$  and 1 indicate the locations of the two recognized vehicles, which are identical to the reference.

In conclusion, our (3-D) optical correlator opens opportunities to process 3-D images directly and rapidly. Therefore, targets distributed in 3-D space can be recognized or tracked by optical correlators in the same fast

and parallel manner as the well-known 2-D correlators have always demonstrated for targets in the 2-D scene.

**References**

1. J. Rosen, "Three dimensional electro-optical correlation," J. Opt. Soc. Am. A **15**, 430-436 (1998).
2. J. Rosen, "Three dimensional joint transform correlator," Appl. Opt. **37** (32), 7538-7544 (1998).

**Diffraction Tomography of Strongly Scattering Objects Based on Homomorphic Filtering**

J.D. Sanchez, A.E. Morales-Porras, M. Testorf, and M.A. Fiddy, Dept. of Electrical & Computer Engin., Univ. of Massachusetts-Lowell, Lowell, MA.

Inverse scattering from far-field data typically requires a solution of the integral equation

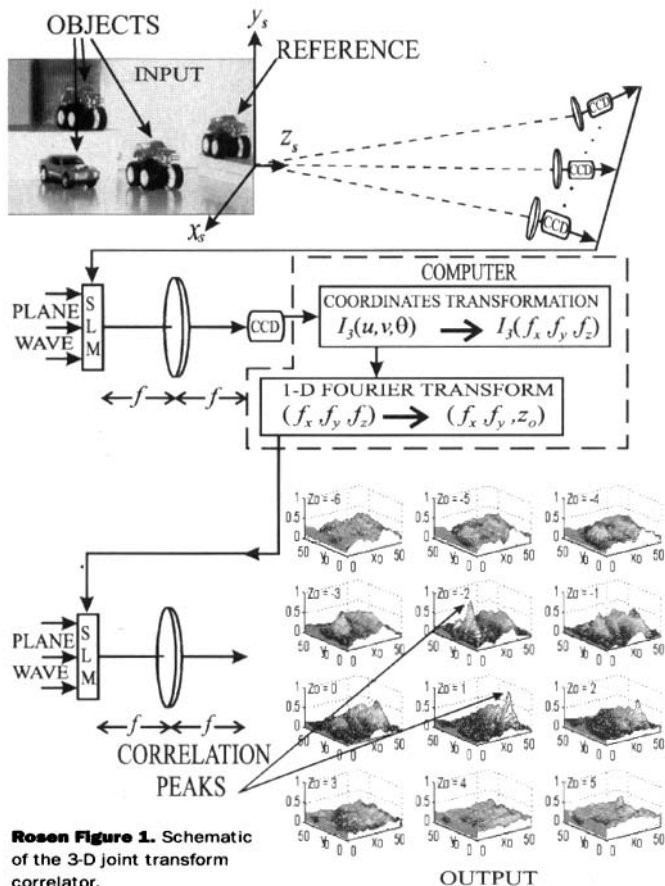
$$\psi_s(\vec{s}_s) = \int V(\vec{r}') \frac{\psi(\vec{r}')}{\psi_i(\vec{r}')} \exp[-ik_0(\vec{s}_s - \vec{s}_i) \cdot \vec{r}'] d^3r', \quad (1)$$

which relates the scattered field  $\psi_s$  to the unknown object  $V^1$ . Here,  $\psi_i = \exp[-ik_0 \vec{s}_i \cdot \vec{r}']$  is the incident field assumed to be a plane wave,  $\psi_s$  is the scattered far field, and  $\psi$  is total field. The unit vectors  $\vec{s}_i$  and  $\vec{s}_s$  describe the propagation direction of incident and scattered field components, respectively.

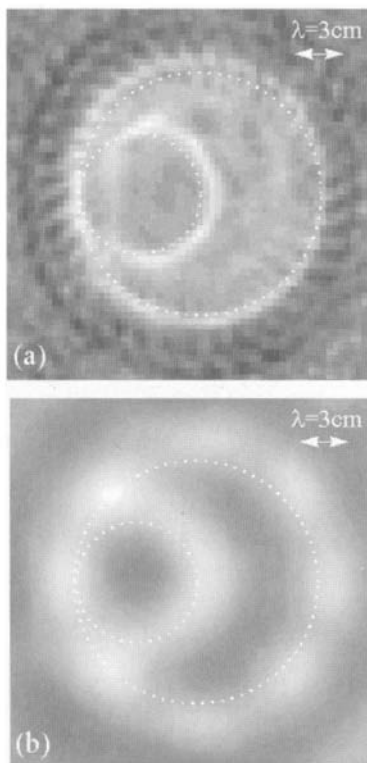
For very weak scattering objects the first Born approximation can be applied, which assumes  $\psi \approx \psi_i$ . Then Eq. 1 identifies  $\psi_s$  as the Fourier transform of the object  $V$  along a circle tangent to the origin in Fourier space. The superposition of data taken with different  $\vec{s}_i$  yields the information about a low pass filtered image of  $V$ . To extend the range of objects that can be imaged, many attempts have been made to evaluate higher-order terms of the Born series approaching the solution of Eq. 1 by means of iterative numerical methods. However, without significant further sophistication, the convergence of the Born series, and hence the validity of reconstruction methods based on it, is still limited to objects with small  $k_0 Va$ , with "a" being a measure of the physical extent of  $V$ .

To image objects with  $k_0 Va \gg 1$ , we chose a different approach based on homomorphic filtering.<sup>1</sup> As an initial step this involves back-propagation of the scattered field  $\psi_s$  for each view that yields an estimate of  $V$  multiplied with  $\psi/\psi_i$ . To remove the field component we take the logarithm to transform the product into a sum. In the cepstral domain, i.e., the Fourier space of the signal's logarithm, we apply a filter. The inverse Fourier transform of the cepstrum is exponentiated. An enhanced estimate of the object is obtained from a superposition of all viewing angles. Cepstral filtering was introduced to remove multiplicative noise.<sup>2</sup> In fact, the only assumption we implicitly make is that the field component is not correlated with the object's structure and the spatial frequency content of both components are substantially different. Both assumptions are at least fulfilled to a certain degree.

Our method was successfully applied to real data problems. Figure 1 shows the reconstruction from data of the Ipswich experiment,<sup>3</sup> which provides the com-



Rosen Figure 1. Schematic of the 3-D joint transform correlator.



**Sanchez Figure 1.** Reconstruction of objects from the Ipswich experiment: (a) IPS007 ( $k_0 Va < 0.01$ ) and (b) IPS008 ( $k_0 Va \approx 50$ ). Both targets have the same geometry (dotted lines), but different permittivity.

munity with the possibility to test imaging methods on experimental microwave data. Figure 1a is the image of the IPS007 object that can be recovered comparatively easy using the Born approximation. The IPS008 object with the same geometry but  $k_0 Va \approx 50$  represents a challenge for the whole community. Figure 1b, in fact, is a state-of-the-art reconstruction.

On the one hand, Figure 1b illustrates that a further sophistication of our method is necessary to permit quantitative imaging with acceptable resolution of strongly scattering objects. On the other, a comparison with competitive methods<sup>4</sup> proves that homomorphic filtering is a very promising approach to inverse scattering. It also supports our belief that signal processing techniques

are well suited to provide fast, reliable, and numerically stable alternatives to iterative reconstruction methods.

### Acknowledgment

M.A. Fiddy and J.D. Sanchez acknowledge the support of Naval Research grant N00014-89-J-1158.

### References

1. J.B. Morris *et al.*, "Nonlinear filtering applied to single view backpropagated images of strong scatterers," *J. Opt. Soc. Am. A* **13**, 1506–1515 (1996).
2. A.V. Oppenheim and R.W. Schaffer, *Digital Signal Processing* (Prentice-Hall, London, U.K., 1975), Chapter 10, pp. 480–531.
3. Measured data provided by the Electromagnetic Technology Division, AFRL/SNH, 31 Grenier St., Hanscom AFB, MA 01731–3010 (Ftp: ercthp1.rl.ph.af.mil).
4. D.A. Pommet *et al.*, "Imaging of unknown targets from measured scattering data," *IEEE AP Magazine* (1998), (accepted).

### Application of Smart Pixels to Optical Implementation of the Wavelet Transform

B. Shoop, D.M. Litynski, and D. Hall, U.S. Military Acad., West Point, NY; P. Das, ECSE Dept., Rensselaer Polytechnic Institute, Troy, NY; C. DeCusatis, IBM Corp., Poughkeepsie, NY.

**T**he concept of wavelets is based on fundamental ideas in transform domain processing, which were first expressed centuries ago in a variety of forms. However, it is only within the past decade, since the pioneering work of Daubechies demonstrated the relationship between wavelets and subband transforms, that significant progress has been made in applying wavelet theory

to practical signal processing problems. Since then, there has been an explosion of interest in wavelets and subband transforms for wide-ranging applications in signal processing, communications, biomedical techniques, and many interdisciplinary fields.<sup>1, 2</sup> The wavelet transform can be implemented using any type of real-time optical correlator. Many optical architectures have been proposed for implementation of the wavelet transform; most of these are based on the Vander Lugt 4-f correlator, the joint transform correlator, or its derivatives such as the quasi-Fourier transform joint transform correlator.<sup>1, 2</sup> We propose to use the advantages of both optics and electronics by demonstrating the use of a smart pixel array as a reflective spatial light modulator (SLM) when implementing the wavelet transform architecture.

Smart pixels are a relatively new technology that closely integrates silicon electronic circuitry and optical devices on a common chip.<sup>3, 4</sup> A 2-D array of smart pixels, which potentially includes optical sources and modulators, detectors, and electronic gain or signal processing functions, can provide both electrical and optical inputs and outputs. The use of smart pixels as a high-speed, programmable SLM is well-suited to a broad range of signal processing problems. There have been many proposed fabrication methods for smart pixels, including monolithic integration, direct epitaxy, epitaxial liftoff, and other hybrid techniques. In particular, liquid crystal on silicon (LCOS) is a hybrid approach with tremendous potential for smart pixel applications.

As illustrated in the cross-section view of Figure 1 (page 48), electronic circuitry is first fabricated on a conventional complimentary metal oxide silicon (CMOS) substrate, including regularly spaced metal contact pads on the chip surface. A cover glass coated with a transparent conductive material such as indium tin oxide (ITO) is then placed on polysilicon spacers and mounted on top of the silicon circuitry (alternately, the cover glass may be mounted atop the natural contours of the processed circuitry). This creates a cavity between the cover glass and the silicon circuitry, which is filled with liquid crystal material. A thin layer of obliquely evaporated silicon monoxide or rubbed polyvinyl alcohol is deposited on the ITO; this makes contact with the liquid crystal material and induces spatial alignment of the liquid crystal molecules.

The liquid crystal is thus in contact with both the alignment layer beneath the conductive coating on the glass and the metal pads on the silicon circuitry. An electric field between these two defines individual pixels at the location of the metal pads. If the pixels are then illuminated, modulation of the electric field results in a corresponding modulation of the phase, intensity, or polarization of the optical signal. In practice, a polarized optical beam is imaged through the liquid crystal onto the metal pads, which also act as high-reflectivity mirrors for the modulated optical beam. In the case of photodetectors, the liquid crystal is not dynamically modulated and the incident optical beam is simply absorbed by the silicon detector.

For a proof-of-concept demonstration, an  $8 \times 8$  LCOS smart pixel array was fabricated on a common substrate